INVESTIGATION OF ELEVATION BIAS OF THE SRTM C- AND X-BAND DIGITAL ELEVATION MODELS

K. Becek

UBD, Geography Department, Jalan Tungku Link, Gadong, BE1410, Brunei Darussalam - kbecek@fass.ubd.edu.bn

ABSTRACT:

The paper presents results of a comparative study of the vegetation-caused elevation bias of the space shuttle topographic mission data product, both C- and X-band (SRTM.C/X). The SRTM.C/X bands data were compared against a high-resolution digital terrain model. Pixel-based differences in SRTM.X minus SRTM.C were correlated with land cover ('agriculture', 'house', 'tree', 'water'). Findings of the investigations include that the SRTM.X does not represent a canopy top of vegetation and that the X-band penetrates deeper vegetation cover than the C-band. As a test site, an area of about 159 km^2 on the Gold Coast, Queensland, Australia, was selected. The area of interest is about 57% covered by vegetation varying from grassland and shrubs to forest. The study method allowed the development of a statistical model relating the elevation bias to the percentage of the vegetation cover of a given land parcel. This model, once verified on varieties of vegetation types, could be utilised to estimate and eliminate the elevation bias from the InSAR elevation model. This model could also be utilised for estimating biomass quantities and their variations. It is hoped that the results will also stimulate investigations towards developing a multi-frequency InSAR system for collecting both terrain elevation data and attributes of biomass.

1. INTRODUCTION

The shuttle radar topography mission elevation data product (SRTM) is one of the most valuable global resources of topographic data to date (Rabus, et al., 2003). It was developed for about 80% of the global landmasses using C-band (λ = 5.3 cm or f = 5.7 GHz) InSAR (interferometry synthetic aperture radar) technology. The vertical (absolute) accuracy is quoted at ±3.3 m – 7.3 m (Rodríguez, et. al., 2005). Pixel size for the U.S. territories is one arc-second (~30 m), and for the remainder of the globe three arc-second (~90 m). The second instrument flown during the same *Endeavour* mission (February, 2000) used the X-band electromagnetic spectrum (λ = 3.1 cm or f = 9.7 GHz), but without the so-called scan mode which provided the data for selected areas of the globe only. These data are available at one arc-second pixel size (~30 m) at a cost of €400 for 15' by 15' tile. Both elevation data products (note neither DTM nor DEM) exhibit elevation bias due to the partial penetration of vegetation by the electromagnetic waves at those bands (C and X). The effect will be referred to as impenetrability of vegetation cover. The level of impenetrability is the layer of vegetation above the ground which is not penetrable by the C- or X-band. The magnitude of the impenetrability depends on many factors related to complex interactions between electromagnetic waves and the 3D object—the vegetation cover. The current scientific position is that the C-band penetrates the vegetation (forest) to about 50% of its thickness, whereas the X-band is reflected from the top of the tree canopy (Carabajal et al., 2006; Balzter et al., 2007). This position seems to be contradicted by at least a few authors who demonstrated that C/X-band impenetrability may be very similar (Werner et al., 2005; Simard et al., 2006). Moreover, it will be shown that the X-band impenetrability can be smaller than the C-band. These inconsistencies are most likely caused by the size, shape, and orientation of scatters within the tree canopy, and can theoretically be used for quantitative assessment of vegetation or biomass. Quantitative assessments of vegetation structure using SRTM data were studied by (Kellndorfer et. al., 2003), who considered determination of vegetation height, using for reference the 'bald-Earth' elevation and SRTM error mitigation procedure. Walker et al., 2007, considered the quality of the SRTM C- and X-band elevation data and their suitability for retrieval of the vegetation canopy height. Balzter et al., 2007, experimented with an airborne L-band and derived and smoothed the 'bald-Earth' elevation model and X-band canopy height. The reported accuracy of that experiment is remarkably high probably because of the relatively flat test site.

In this paper, the impenetrability of vegetation cover is investigated. The test site, located in Australia, consists of various types of land cover, varying between grassland, urban, and tree cover with various densities. The main goal of the investigation is to document the existence of situations where X-band impenetrability is less than that of C-band, or in other words, when X-band microwaves penetrate the vegetation cover deeper than C-band waves. An attempt is also made to relate the difference in impenetrabilities to the height, density, and type of vegetation cover. Answers to those questions can lead to the development of a multifrequency (C/X/L-band) microwave system for mapping the vertical structure of vegetation cover.

2. MATERIAL AND METHODS

2.1 Test site

The test site comprises the northern part of Gold Coast City, Queensland, Australia (top left: 153.25 E, 23.75 S, and bottom right: 153.5 E, 28 S). All water bodies were masked out from further consideration. The area of the considered terrain was about 153.9 km^2. A sun-shadowed view of the test site is shown

Figure 1. Sun-shadowed view of the test site, Gold Coast City, Queensland, Australia.

in Figure 1. The geomorphology of about half of the site is composed of low, flat alluvia; the remainder is formed by eroded hills and valleys of volcanic origin.
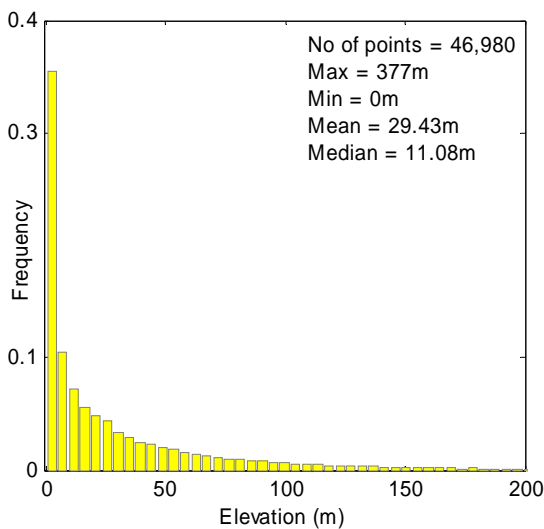

Figure 2. Histogram of elevations of the test site.

The highest point is about 377 m a.m.s.l. The mean and median elevations are about 29 m and 11 m, respectively. Figure 2 shows a histogram of the terrain's elevation, which resembles an exponential distribution. The degree of the terrain's roughness can be seen in Figure 3. The mean slope for AOI is about 3°, which is classified as flat terrain.

The AOI land cover can be divided into four land cover classes, e.g., a) agricultural land (predominantly under sugar cane and pastoral areas); b) trees and shrubs usually forming dry rainforest and open eucalyptus forests of grey gum (*Eucalyptus punctata*) open-crowned tree, blue gum (*Eucalyptus tereticornis*), and stringybark and tallowwood (*Eucalyptus microcorys*) trees. Mean tree height is about 20 m, but it can reach 45 m in instances; c) high-density housing estates with

very low to none tree cover; and d) water bodies in the form of small dams or lakes, and artificial channels connected to rivers. Land cover of about 10%, 57%, 19%, and 14% constituted classes a, b, c, and d, respectively.
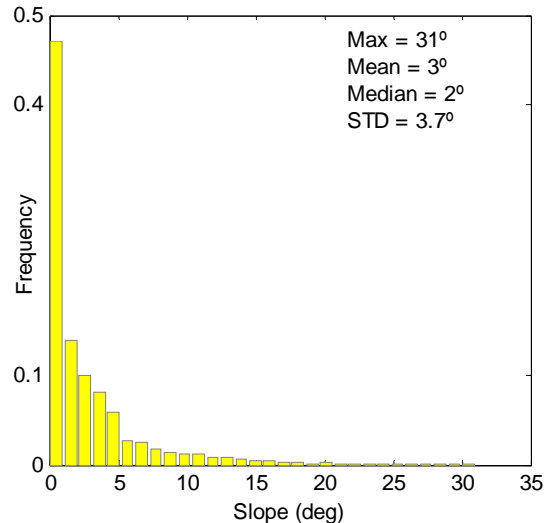

Figure 3. Histogram of the terrain's slopes of the test site.

2.2 Data

SRTM Data

The SRTM.C, so-called finished data, version 2 (cell S28E153.hgt.zip) were downloaded from the JPS/NASA site: ftp://e0srp01u.ecs.nasa.gov/srtm/version2/SRTM3/Australia/. This is the recommended source of the SRTM.C because its three arc-second downsampling has been achieved using the so-called averaging procedure (Becek, 2007). A 15 arc-minute SRTM.X one arc-second cell (starting at 153.25 E, 28.0 S – bottom left corner) has been purchased from the German Aerospace Center (DLR). All pixels falling within water bodies were removed. Every pixel from the SRTM.X data set was associated with the so-called height error map value (HEM), a pixel-based accuracy measure provided as a part of the X-band data package. The HEM value is statistically determined from a neighbourhood of pixels mainly considering the phase and baseline stability. Thus, it is a relative measure of the precision. The HEM varies in a range from 0 to 255. The C-band elevations are referred to the sea level means. The X-band ellipsoidal elevation was converted to mean sea level using the AusGeoid98 model http://www.ga.gov.au/geodesy/ausgeoid/. The C-band pixels were also associated with an accuracy measure derived from the slope of the terrain. In the following section, a procedure facilitating that is described.

DTM Data

As reference terrain elevation data, a set of spot elevations was used. The accuracy of the photogrammetically/lidar derived elevations is better than ± 0.3 m (1 σ). The mean density of the spot elevations was about 48 points /ha.

Land Cover Data

The Digital Cadastral Data Base (DCDB), one of the standard 'spatial' products available in Queensland, Australia, at minimal cost, was used for parcel-based land cover classification. By means of photointerpretation of high-resolution 2003 aerial photography (0.15-m pixel), about 71,500 land parcels were classified as 'Agriculture', 'House', 'Water', and 'Tree'. The 'Tree' parcels were also assigned visually assessed percentages of tree cover. Figure 1 shows DCDB in the background of an aerial photograph.

Figure 4. Parcel-based classification of land cover including the percentage of tree cover. 'A' denotes 'Agriculture', 'H' – 'House', 'T35' – 35% of 'tree' cover, and 'W' – 'water'.

2.3 Method

In the following, the data processing procedure will be presented. As a basic unit for calculations and data aggregations, a buffer with a 45-m radius centred on the centre of every C-band pixel was used. For every such buffer, the following data were available:

a) Average X-band elevation (calculated from up to 12 points),
b) Average reference elevation (calculated from 13.3 (1 -108) - in average - reference spot elevations,
c) Type of land cover,
d) Percentage of tree cover,
e) Aspect calculated from C-band data,
f) Slope calculated from C-band data,
g) HEM value for X-band pixels, and
h) A pixel based accuracy of C-band elevations.

Buffers with missing data in any field or containing SRTM.X pixels with HEM>10 were omitted from further processing. Overall, 53,190 buffers were available for further processing. Data preparation also included identification of horizontal mis-registration of both C- and X band data in relation to the reference DTM. This was performed by calculating the cross-correlation plot for two perpendicular transects (N-S and E-W). No shift was detected at the lag level of 2.5 m. In the next step, the differences in elevations between SRTM and reference DTM for every buffer were calculated:

$$
\begin{aligned}
dC &= C - \langle R \rangle, \\
dX &= \langle X \rangle - \langle R \rangle, \\
dCX &= C - \langle X \rangle
\end{aligned}
\tag{1}
$$

where dC, dX, dCX = difference in elevation, C, X and R = C-, X-band elevations, and R is the reference elevation,

$\langle \ \rangle$ = spatial (buffer) averaging operator.

Variation of difference (σ_d^2) was calculated for every buffer as a sum of the variations of the C/X-band ($\sigma_{C/X}^2$) and variations of the reference elevation (σ_R^2):

$$
\sigma_d^2 = \sigma_{C/X}^2 + \sigma_R^2
\tag{2}
$$

The pixel-based variation of the C/X-band data ($\sigma_{C/X}^2$) was calculated as a sum of the variation of the SRTM instrumental error and error caused by impenetrability in conjunction with C/X - pixel size (Becek, 2008):

$$
\sigma_{C/X}^2 = 1.55^2 + 1/12 * d^2 * \tan^2(s)
\tag{3}
$$

where d = 30 m or 90 m for X- or C-band pixel
s = slope of terrain within a pixel, and
1.55 m is an experimentally derived standard deviation of the instrumental errors of the SRTM.

In the next step, using a reciprocal of the variance (2) as the weight, the weighted average differences dCw, dXw, dCXw, and their standard deviations were calculated for every parcel (belonging to one of the land cover classes). The calculations were done using well-known formulas:

$$
d(.)w_i = \left\langle \frac{\sum d(.)g}{\sum g} \right\rangle_i
\tag{4}
$$

$$
g = 1/\sigma_d^2
\tag{5}
$$

where $d(.)w_i$ = weighted difference dC, dX, or dCX for i-th parcel

$\langle \ \rangle$ = spatial (parcel) averaging operator.

The standard deviation of the average difference (Equation 4) can be calculated using the following formula:

$$
\sigma_d^2 = \sigma^2 / \sum g
\tag{6}
$$

Where σ = the standard deviation of an average difference with the weight equal to 1, and
g = weight (Equation 5).

Calculated average differences for every parcel were subsequently analysed as a function of the land cover.

3. RESULTS

The vegetation impenetrability and anthropogenic obstructions found above the surface of the Earth introduce asymmetry into the histogram of elevation differences (SRTM minus 'bald-Earth' reference elevations) (Heipke, et al., 2002). Histograms in Figure 5, 6, and 7 were developed for vegetation impenetrabilities (Equation 2). The mean differences for SRTM.C/X minus the reference elevation are 6.62 m and 2.53 m, respectively. Hence, the mean difference for SRTM.C minus SRTM.X is about 4 m.
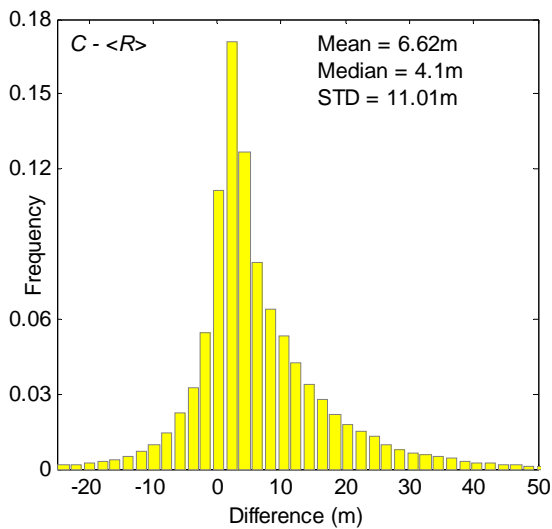

Figure 5. Histogram of buffer-based elevation differences C-band minus reference elevation.
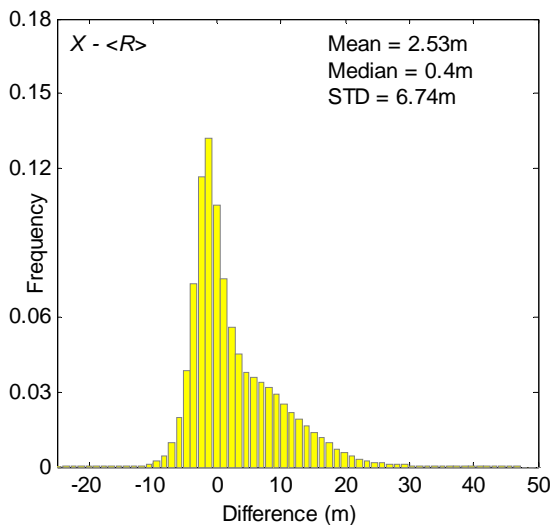

Figure 6. Histogram of buffer-based elevation differences X-band minus reference elevation.

The histograms in Figures 5 and 6 do not follow the Gaussian-fitting curve. This is because they represent a compound probability distribution function of two stochastic processes: one is the 'bald-Earth' difference between SRTM and reference DTM, which follows the Laplace distribution; the second one is created as the same difference but considered over vegetated areas—it follows the Gaussian distribution. The Gaussian probability density function is given by the well-known formula:

$$f(x|m,\sigma) = \frac{1}{\sigma\sqrt{2\pi}} e^{-0.5\left(\frac{x-m}{\sigma}\right)^2}, \tag{7}$$

where m = mean value, and
σ = standard deviation.

The Laplace probability density function is given by (Norton, 1984):

$$f(x|\mu,b) = \frac{1}{2b} e^{\left(-\frac{|x-\mu|}{b}\right)}, \tag{8}$$

where μ = location parameter,
b = scale parameter.

For N independent and identically distributed differences d_1, d_2, ..., d_N, estimator of μ - $\tilde{\mu}$ is the median of differences, and the estimator of b - $\tilde{b}$ can be calculated using the maximal likelihood estimator from:

$$\tilde{b} = \frac{1}{N}\sum_{i=1}^{N}|d_i - \tilde{\mu}|, \tag{9}$$
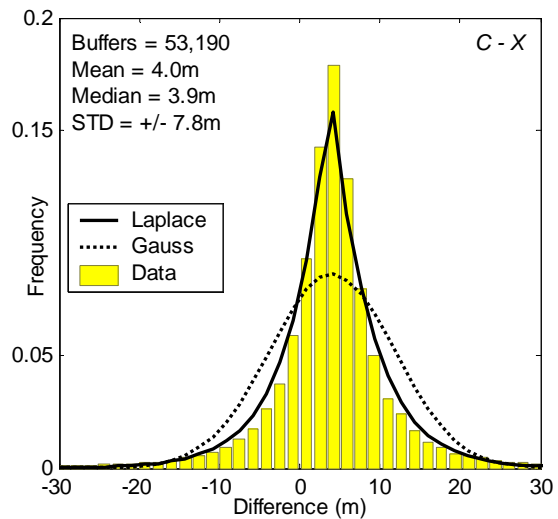

Figure 7. Histogram of differences C-band minus X-band.
Laplace fitting curve was drawn for μ = 3.9 m and b = 4.96 m.
Gaussian fitting curve was drawn for m = 4.0 m and σ = ±7.8 m.

The difference *dCX* for the whole AOI shown in Figure 7 follows the Laplace distribution. The mean difference is 4.0 m, which means that the X-band vegetation impenetrability is less than the C-band one.
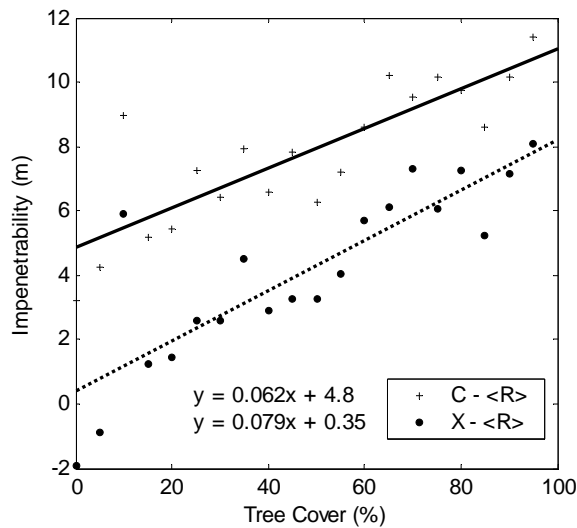

Figure 8. Impenetrability of the C/X-band versus percentage of the parcel-based tree cover.

A potentially far-reaching consequence for vegetation cover investigations is the relationship between SRTM bias and the percentage of vegetation cover of a given area. This effect is illustrated in Figure 8. For example, any future changes to vegetation cover in terms of spatial extensions (horizontal and vertical) can be easily identified by comparing multi-temporal C- or X-band impenetrability of a given area. However, it is necessary to note that the data for the C-band vegetation impenetrability shown in Figure 8 indicate about 4.8 m positive bias (SRTM is above the ground) for the vegetation-free parcels. This issue will be further investigated in the near future.

Differences *dC* and *dX,* or elevation bias, are shown in Table 9.

Land Cover Class	Difference (m)	
	$dC \pm 1\sigma$	$dX \pm 1\sigma$
Agriculture	2.96 ± 3.56	-1.46 ± 1.49
House	4.24 ± 7.12	0.28 ± 4.18
Tree (0-100%)	8.29 ± 9.97	3.69 ± 6.27
Water	4.34 ± 6.82	0.32 ± 4.54

Table 9. SRTM C/X elevation bias for land cover classes

Closer consideration of the results in Table 9, in particular for 'Agriculture,' can lead to a conclusion that perhaps both C- and X-band SRTM datasets contain certain reference biases, e.g., C-band elevations are about 3 m too high, and X-band elevations are about 1.5 m too low. This could explain the remarks regarding the 4.8-m bias made in the previous paragraph. The negative X-band SRTM elevation bias of the order of about 2.6 m was reported by Heipke et al., 2002. However, Ludwig et al., 2006, have not reported such an elevation bias.

Weighted average difference *dCXw* per Equation 4 was calculated for every land cover type. The results are very similar, varying between 3.95 m for 'House' and 4.43 m for

'Agriculture' and 'Trees'. The standard deviation varied between ±2.79 m for 'Agriculture' and ±6.88 m for 'Trees'.
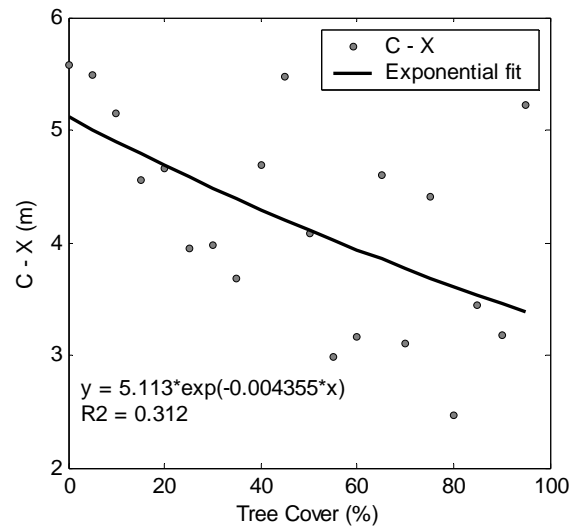

Figure 10. Weighted average difference SRTM.C minus SRTM.X versus tree cover expressed as a percentage of the area of the parcel.

The weighted average difference *dCXw* for 'Tree' was also calculated for every parcel as a function of the average percentage of tree cover. The results are shown in Figure 10. The data appear to follow the exponential fitting curve. The difference is that *dCXw* reaches its lowest level of about 3.3 m for parcels fully covered by trees. The relatively low value of R^2 is mainly caused by inexperienced photointerpreters who estimated the percentage of the tree cover.

4. CONCLUSIONS

A comparison of both C- and X-band SRTM elevation products and a high-resolution reference DTM over a large test area in the Gold Coast, Queensland, Australia, focused on the influence of the vegetation cover, which was in the leave-on state, on elevation bias and provided an inside look into some of the properties of the InSAR C- and X-band technology of elevation determination. There is evidence that the X-band SRTM penetrates the vegetation cover deeper than the C-band SRTM. This effectively means that the vegetation-caused error in the X-band SRTM is smaller than that in the C-band SRTM. However, this has to be further investigated due to possible systematic error in the C-band SRTM.

It was also shown that there is a linear relationship between the percentage of land cover and the magnitude of the vegetation-caused bias. This property of both SRTM datasets can be utilised for quantitative observations of variations of vegetation cover.

The level of the vegetation-caused impenetrability, e.g., about 10 m, is responsible for an error exceeding SRTM mission error specification. In addition, this is valid for about 30% of the global landmasses covered by forests.

Further investigations are needed and planned towards identifying the best data source of vegetation cover to be used

to correct the SRTM elevation data product and those which will be derived in the future using the InSAR technology.

REFERENCES

Balzter, H., Rowland, C.S. & Saichc, P., 2007. Forest canopy height and carbon estimation at Monks Wood National Nature Reserve, UK, using dual-wavelength SAR interferometry. *Remote Sensing of Environment*, 108(3), pp. 224-239.

Becek, K., 2006. Accuracy Evaluation of the SRTM Topographic Data Product over Selected Sites in Australia and Brunei Darussalam. *Reports on Geodesy*, 77(2), pp. 283-289.

Becek, K., 2007. Comparison of Decimation and Averaging Methods of DEM's Resampling. Proceedings of the Map Asia 2007 conference, Kuala Lumpur, http://www.gisdevelopment.net/technology/ip/ma07267.htm (accessed – March 2008).

Becek, K., 2008. Investigating Error Structure of SRTM Elevation Data Product. *Submitted to the Geophysical Research Letters*.

Carabajal C.C. & Harding, D.J., 2006. SRTM C-band and ICESat Laser Altimetry Elevation Comparisons as a Function of Tree Cover and Relief. *Photogrammetric Engineering & Remote Sensing,* 72(3), pp. 287-298.

Gesch, D., 2005. Vertical Accuracy of SRTM Data of the United States: Implications for United States: Implications for Topographic Change Detection. SRTM Data Validation and Applications Workshop June 14, 2005, http://edc.usgs.gov/conferences/SRTM/presentations/Slides06_Gesch.pdf (accessed - April 2008)

Heipke, C., Koch, A. & Lohmann, P. 2002: *Analysis of SRTM DTM - Methodology and practical results.* Proceedings of ISPRS Commission IV Symposium in Ottawa, July 2002.

Kellndorfer, J.M., Walker, W.S., Pierce, L.E., Dobson, M.C., Fites, J. Hunsaker, C., Vona, J., Clutter, M, 2004. Vegetation Vegetation height derivation from height derivation from Shuttle Radar Topography Mission and National Elevation data sets. *Remote Sensing of Environment*, 93(3), pp. 339-358.

Ludwig, R., & Schneider, P. 2006. Validation of digital elevation models from SRTM X-SAR for applications in hydrologic modeling. *ISPRS Journal of Photogrammetry and Remote Sensing*, 60(5), pp.339-358.

Norton, R.M., 1984. Double Exponential Distribution: Using Calculus to Find a Maximum Likelihood Estimator. *The American Statistician*, 38(2), pp. 135-136.

Rabus, B., Eineder, M., Roth, A., & Bamler, R., 2003. The shuttle radar topography mission—a new class of digital elevation models acquired by spaceborne radar. *ISPRS Journal of Photogrammetry and Remote Sensing*, 57(4), pp.241-26.

Rodríguez, E., Morris, C.S., Belz, J.E., Chapin, E.C., Martin, J.M., Daffer, W., & Hensley, S., 2005. An assessment of the SRTM topographic products. *Technical Report JPL D-31639, Jet Propulsion Laboratory, Pasadena, California,* 143 pp.

Schumann, G., Matgen, P., Cutler, M.E.J., Black, A., Hoffmann, L., & Pfister, L., 2007. Comparison of remotely sensed water stages from LiDAR, topographic contours and SRTM. *ISPRS Journal of Photogrammetry and Remote Sensing*, *(2007)*.

Simard, M., Zhang, K., Rivera-Monroy, V.H., Ross, M.S., Ruiz, P.L., Castañeda-Moya, E., Twilley, R.R. & Rodriguez, E., 2006: Mapping Height and Biomass of Mangrove Forests in the Everglades National Park with SRTM Elevation Data. *Photogrammetric Engineering & Remote Sensing*, 72(3), pp. 299-311.

Walker, W., Kellndorfer, J. & Pierce, L. 2007. Quality Assessment of SRTM C-and X-band Interferometric Data: Implications for the Retrieval of Vegetation Canopy Height. Remote Sensing of Environment, 106(4) pp 428-448.

Werner, M., Roth, A., Marschalk, U., Eineder, M. & Suchandt, S. 2005. Comparison of DEMs derived from SRTM/X-and C-Band. *Workshop: "The Shuttle Radar Topography Mission – Data Validation and Applications"*, June 14-16, 2005, Reston, Virginia, USA.